Finite Time Adaptive Smooth Non Linear Sliding Mode Control for Second Order Dynamic Systems

José Antonio González-Prieto (jagprieto@gmail.com)

Centro Universitario de la Defensa en la Escuela Naval Militar de Marín https://orcid.org/0000-0002-7099-6590

Research Article

Keywords: Finite Time, Super-Twisting, Adaptive, Smooth Non Linear, Sliding Mode, Peaking, Chattering

Posted Date: January 19th, 2022

DOI: https://doi.org/10.21203/rs.3.rs-1241962/v1

Noname manuscript No.
(will be inserted by the editor)

Finite Time Adaptive Smooth Non Linear Sliding Mode Control for Second Order Dynamic Systems

Adaptive Smooth Non Linear Super-Twisting Approximation

José Antonio González-Prieto

Received: date / Accepted: date

Abstract In this paper, a feedback control law that employs an adaptive smooth nonlinear approximation of the Super-Twisting (STW) algorithm is presented in order to generate a smooth control law capable of regulating in finite time a second-order system that is affected by unknown disturbances and uncertainties. A nonlinear sliding surface is created in order to set the desired dynamics of the response, so that the control law is proposed to establish global properties of stability for unperturbed and perturbed systems. More specifically, the method entails determining parameters that eliminate chattering in noise-free models by means of a simple cut-off frequency design parameter approach. Therefore, the methodology is characterized by its simplicity and robustness. A second order mechanical system is used to demonstrate the effectiveness of the proposed algorithm.

Keywords Finite Time · Super-Twisting · Adaptive · Smooth Non Linear · Sliding Mode · Peaking · Chattering

1 Introduction.

Sliding Mode Control (SMC), [1, 2, 3, 4, 5, 6, 7, 8, 9, 10, 11, 12, 13, 14, 15, 16, 17, 18], is one of the approaches has been proposed in the literature in order to make control robust to disturbances and uncertainties. The traditional sliding mode control, also called first-order sliding mode control, is characterized by a saturated and discontinuous control input. Based on this approach multiple solutions have been provided, with some proposals of advanced sliding manifolds including recursive nonlinear sliding manifolds [19, 20, 21, 22], adaptive integral sliding mode approach [23, 24, 25], non linear full order dynamics [26, 27], sliding surfaces with adaptive damping parameters [28, 29, 30], integration with neural and fuzzy networks [31, 32] and, in the last years, a

José Antonio González-Prieto at Centro Universitario de la Defensa,
Escuela Naval Militar, Marín 36920, Galicia, Spain (e-mail: jose.gonzalez@cud.uvigo.es)

vast collection of homogeneity based works, see [33] for instance. Applications of the properties of homogeneous systems is an important field of study in the current development of analysis and design of nonlinear controllers and observers.

In nonlinear control systems, homogeneity simplifies analysis and design as the homogeneous vector fields exhibit many properties similar to linear ones and provide solutions with finite-time stability as well as fixed-time stability. The dynamics generated by an homogeneous controller can be seen as a lineal dynamic system with an adaptive gain that grows to ∞ as $|x(t)| \to 0$, generating the well know singularity at the origin which is undesired for real applications.

In spite of this, as pointed out in [34], the practical implementation of homogeneous dynamics systems that are designed in continuous time domains prevents the use of explicit *Euler* discretization schemes to achieve a mere replica of continuous time. Discretization of this type is considered inappropriate, especially when set-valued functions are to be accounted for, resulting in numerical chattering and sensitivity to gains. Due to this, comparisons between set value and homogeneous solutions with other types of proposals may lead to unfair conclusions without addressing the discretization issue.

The STW is a well-known second order sliding mode ($SOSM$) algorithm that has been widely applied in control and observation, [35, 36, 37, 38, 39, 40, 41, 42, 43]. As related dynamics are discontinuous, its solutions are interpreted in the sense of *Filippov*, so that selection of an adequate values for the algorithm gains can be a difficult problem in practical applications, mainly due to two issues: the peaking and chattering phenomena.

The *peaking phenomenon* appears in linear systems when it is needed to implement high-gain feedback laws that leads to produce eigenvalues with a large negative part, [44]. Therefore, certain states peak to very large values before they decay to zero, such that these states may destabilize the system and even make certain states reach infinite values in finite escape time.

Chattering phenomenon constitutes high-frequency, finite-amplitude oscillations [45]. The two possible causes of chattering in steady-state responses are: the use of non-continuous functions, such as the set-valued sign function that is used in classical sliding mode controls, and discretization, which may introduce chattering in the steady-state response if the gains are large enough, even if all the functions are smooth, provided the system dynamics are characterized by high frequency components with respect to the sampling time τ.

Based on the aforementioned results, in order to keep the discretization process simple, an adaptive smooth nonlinear sliding mode surface law is introduced in this work. In this case, the dynamics flows with adaptive and finite damper gain, avoiding the effects of the peaking transient response inherent to linear systems and allowing fast responses at steady state, approximating the behaviour obtained with homogeneous solutions. Besides, the adaptation process is based on a cut-off frequency parameter design that, together with the sampling time, determines the properties of the response obtained.

An investigation of a smooth nonlinear approximation definition of the set value sign function can be conducted by using sigmoid functions $\chi(x)$, see [46]. The following conditions must be met by this type of function:

1. The function $\chi(x)$ is smooth.
2. The function $\chi(x)$ is odd.
3. The function satisfies $\lim_{x\to\pm\infty} |\chi(x)| = 1$.

Taken account that:

$$\lim_{\gamma\to+\infty} \tanh(\gamma x) = \text{sign}(x) \tag{1}$$

a parameterized (with γ being the design parameter) hyperbolic tangent function is introduced in this work. Recently, a smooth nonlinear approximation that uses nested sliding surfaces has been introduced in [47] as a framework to design cascade high gain observers. In this work this framework is updated to introduce a Lyapunov based quadratic stability analysis.

This paper has been structured as follows. First, in Section 2 we present a nonlinear smooth approximation of the *STW* algorithm and analyze its asymptotic and finite time stability properties. Then, Section 3 describes the discretization and the parameter design procedure, including an adaptive cut-off frequency domain approach. Section 4 introduces the application of the proposed algorithm considering a control affine second order system by means of the definition of an adaptive non linear sliding mode surface. Results from numerical simulations are then presented and discussed in Section 5. Finally, conclusions are drawn in Section 6.

2 Adaptive Smooth Nonlinear Super-Twisting Approximation.

Consider that an output sliding variable $\sigma(t)$ has been defined for a second order dynamics system, such that it is obtained a first-order dynamical system of the form:

$$\dot{\sigma}(t) = u(\sigma) + d(t) \tag{2}$$

In this case, $u(\sigma)$ is the control input to be designed and $d(t)$ is the unknown (external disturbances and model uncertainties) that satisfies the following assumption

Assumption 21 *$d(t)$ in (2) satisfies the following restriction*

$$|\dot{d}(t)| \leq \Delta$$

with $\Delta > 0$ a positive known real number.

The goal is to determine the input function $u(\sigma)$ such that the value of $\sigma(t)$ converges to the origin. The STW algorithm, see [48, 49, 50], provides the following solution:

$$\begin{aligned} u(\sigma) &= -\lambda\sqrt{|\sigma(t)|}\,\text{sign}\,(\sigma(t)) - \epsilon(t) \\ \dot{\epsilon}(t) &= \kappa\,\text{sign}\,(\sigma(t)) \end{aligned} \tag{3}$$

Let's define $\omega(t)$ as:

$$\omega(t) = d(t) - \epsilon(t) \tag{4}$$

As a result, the dynamics of $\sigma(t)$ and $\omega(t)$ are obtained as:

$$\begin{aligned} \dot{\sigma}(t) &= -\lambda\sqrt{|\sigma(t)|}\,\text{sign}\,(\sigma(t)) + \omega(t) \\ \dot{\omega}(t) &= -\kappa\,\text{sign}\,(\sigma(t)) + \dot{d}(t) \end{aligned} \tag{5}$$

A smooth nonlinear dynamics approximation of STW is proposed in this work as follows:

$$\begin{aligned} u(\sigma) &= -\lambda\sigma(t) - \beta\tanh(\gamma\sigma) - \epsilon(t) \\ \dot{\epsilon}(t) &= \frac{\lambda^2}{4}\sigma(t) + \kappa\tanh(\gamma\sigma) \end{aligned} \tag{6}$$

The set value ($\text{sign}(e(t))$) and the power factor ($|e(t)|^{0.5}$) used in (5) are replaced in (6) with a combination of linear and nonlinear smooth functions with, as it will be shown, adaptive gains that are chosen by means of a cut-off frequency domain criterion. Hence, the algorithm is named as *Adaptive Smooth Nonlinear Super-Twisting Approximation (ASNSTA)*. As a result, the dynamics of $\sigma(t)$ and $\omega(t)$ are obtained as:

$$\begin{aligned} \dot{\sigma}(t) &= -\lambda\sigma(t) - \beta\tanh(\gamma\sigma) + \omega(t) \\ \dot{\omega}(t) &= -\frac{\lambda^2}{4}\sigma(t) - \kappa\tanh(\gamma\sigma) + \dot{d}(t) \end{aligned} \tag{7}$$

2.1 Asymptotic stability analysis.

Let's define $\eta(t)$ as:

$$\eta(t) = \begin{bmatrix}\sigma(t) & \omega(t)\end{bmatrix}^T \tag{8}$$

and parameters $p_i, i = 1, 2, 3$ as:

$$p_1 = \frac{\lambda^2 + 4}{8\lambda} \tag{9}$$

$$p_2 = \frac{5\lambda^2 + 4}{2\lambda^3} \tag{10}$$

$$p_3 = \frac{\lambda^4 + 24\lambda^2 + 16}{8\lambda(5\lambda^2 + 4)} \tag{11}$$

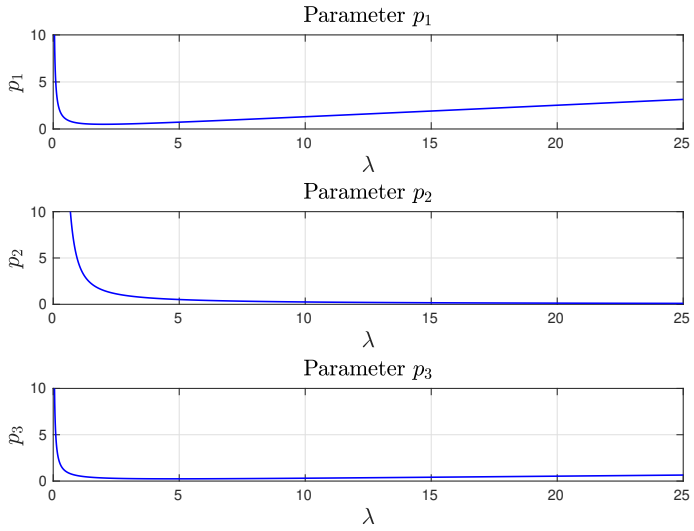

Fig. 1 Parameters p_1, p_2 and p_3 as a function of λ.

Note that $p_3 > 0$ is given as:

$$p_3 = \frac{4p_2p_1 - 1}{4p_2} \tag{12}$$

Figure (1) shows the values of p_1, p_2 and p_3 as function of the value of $\lambda > 0$. Let P, a symmetric positive definite matrix, defined as:

$$P = \begin{pmatrix} p_1 & -0.5 \\ -0.5 & p_2 \end{pmatrix} \tag{13}$$

with determinant $|P|$ given as:

$$|P| = \frac{\lambda^4 + 24\lambda^2 + 16}{16\lambda^4} \tag{14}$$

We first explore stability conditions in the worst case.

Theorem 1 *Define ϕ and κ as follows:*

$$\phi = \sqrt{2}\max(0.5, p_2) \tag{15}$$

$$\kappa = \frac{\beta}{2p_2} \tag{16}$$

The compact set Ω_{η_1} defined as:

$$\Omega_{\eta_1} = \{\eta(t) \in \mathbb{R}^2 : -\frac{1}{2}||\eta|| - \frac{p_3\beta|\tanh(\gamma\sigma)||\sigma(t)|}{||\eta||} + \Delta\phi < 0\} \tag{17}$$

is Globally Uniformly Asymptotically Stable (GUAS).

Proof Dynamics of $\eta(t)$ are given by:

$$\dot{\eta}(t) = A\eta(t) + F(t) + D(t) \tag{18}$$

with

$$A = \begin{pmatrix} -\lambda & 1 \\ -\frac{\lambda^2}{4} & 0 \end{pmatrix} \tag{19}$$

and

$$F(t) = \begin{pmatrix} -F_\sigma \\ -F_\omega \end{pmatrix} = \begin{pmatrix} -\beta \tanh(\gamma\sigma) \\ -\kappa \tanh(\gamma\sigma) \end{pmatrix} \tag{20}$$

$$D(t) = \begin{pmatrix} 0 \\ \dot{d}(t) \end{pmatrix} \tag{21}$$

It can be shown that:

$$PA + A^T P = -I_{2x2} \tag{22}$$

where I_{2x2} is the identity matrix of size 2x2. Choosing a Lyapunov candidate function

$$V(\eta) = \frac{1}{2}\eta^T P \eta \tag{23}$$

leads to

$$\begin{aligned} \dot{V}(\eta) &= -\frac{1}{2}\eta^T\eta + F^T P\eta + D^T P\eta \\ &= -\frac{1}{2}||\eta||^2 + (p_1 F_\sigma - 0.5F_\omega)\sigma(t) \\ &+ (p_2 F_\omega - 0.5F_\sigma)\omega(t) + \dot{d}(t)(p_2\omega(t) - 0.5\sigma(t)) \end{aligned} \tag{24}$$

Equations (16) and (10) implies that:

$$p_2 F_\omega - 0.5F_\sigma = 0 \tag{25}$$

In addition, it implies:

$$p_1 F_\sigma - 0.5F_\omega = (p_1 - \frac{1}{4p_2})F_\sigma = p_3\beta \tanh(\gamma\sigma) \tag{26}$$

Applying these results it is obtained:

$$\begin{aligned} \dot{V}(\eta) &= -\frac{1}{2}\eta^T\eta + F^T P\eta + D^T P\eta \\ &= -\frac{1}{2}||\eta||^2 - p_3\beta|\tanh(\gamma\sigma)||\sigma(t)| + \dot{d}(t)(p_2\omega(t) - 0.5\sigma(t)) \end{aligned} \tag{27}$$

Therefore

$$\dot{V}(\eta) \leq -\frac{1}{2}||\eta||^2 - p_3\beta|\tanh(\gamma\sigma)||\sigma(t)| + \Delta\phi||\eta|| \tag{28}$$

which finalizes the proof.

If λ is high, then p_2 must be small, which reduces the effect of the unknown term $\dot{d}(t)p_2\omega(t)$ on stability performance. It is thus possible to set values of β and λ which guarantee the inclusion of the origin in the domain of asymptotic attraction taking account of the restriction specified by the parameter Δ. For the purpose of creating a closed compact set that includes the origin of $\eta(t)$, the value of β must be defined according to the desired precision. This scenario is described into the following theorem.

Theorem 2 *Let us define ν as:*

$$\nu = \frac{\operatorname{atanh}(\frac{\Delta}{p_3}\frac{(p_2\alpha+0.5)}{\beta})}{\gamma} \tag{29}$$

with $\alpha > 0$ a parameter to be designed. The compact set Ω_{η_2} defined as:

$$\Omega_{\eta_2} = \{\eta(t) \in \mathbb{R}^2 : |\sigma(t)| < \nu \wedge |\omega(t)| < \alpha\frac{|\tanh(\gamma\sigma)|}{\tanh(\gamma\nu)}|\sigma(t)| + \frac{1}{2\Delta p_2}||\eta||^2\} \tag{30}$$

, which is a closed set including the origin of $\eta(t)$, is GUAS.

Proof Equation (29) implies that:

$$\beta = \frac{\Delta}{p_3}\frac{(p_2\alpha + 0.5)}{\tanh(\gamma\nu)} \tag{31}$$

Substitution of (31) into (27) implies:

$$\dot{V}(\eta) = -\frac{1}{2}||\eta||^2 - \Delta\left[0.5(\frac{|\tanh(\gamma\sigma)|}{\tanh(\gamma\nu)} - 1)|\sigma| + p_2(\alpha\frac{|\tanh(\gamma\sigma)|}{\tanh(\gamma\nu)}|\sigma| - |\omega|)\right] \tag{32}$$

Condition $|\sigma| > \nu$ implies $\frac{\tanh(\gamma\sigma)}{\tanh(\gamma\nu)} > 1$, so that it is obtained:

$$\dot{V}(\eta) \leq -\frac{1}{2}||\eta||^2 - \Delta p_2(\alpha\frac{|\tanh(\gamma\sigma)|}{\tanh(\gamma\nu)}|\sigma| - |\omega|)\ \forall|\sigma| > \nu \tag{33}$$

Condition:

$$|\omega(t)| < \alpha\frac{|\tanh(\gamma\sigma)|}{\tanh(\gamma\nu)}|\sigma| + \frac{1}{2\Delta p_2}||\eta||^2 \tag{34}$$

implies that $\dot{V}(\eta) < 0$, which ends the proof.

2.2 Finite Time stability analysis.

We now consider the conditions for achieving Finite Time Stability (FTS). Let us recall the following result first outlined in [51]:

Lemma 1 *For any real numbers $c_1 > 0$, $c_2 > 0$ and $0 < b < 1$, an extended Lyapunov function condition of finite time stability can be given as:*

$$\dot{V}(x) + c_1 V(x) + c_2 V^b(x) \leq 0 \tag{35}$$

where the settling time can be estimated by:

$$T \leq \frac{1}{c_1(1-b)} \ln\left(\frac{c_1 V^{(1-b)}(0) + c_2}{c_2}\right) \tag{36}$$

Furthermore, let us introduce two useful nonlinear inequalities that can be applied to the smooth nonlinear approximation methodology.

Lemma 2 *Let $0 < \delta < 1$, then the following conditions holds:*

$$\delta|\sigma| + (1-\delta) \geq |\sigma|^\delta \tag{37}$$

Proof The top plot of Figure (2) displays the geometrical construction of the proposed inequality. Taking $\sigma = 1$ as the desired root of the inequality, a line must be traced from position $(0, 1-\delta)$ to position $(1, 1)$ in order to achieve condition (2). The slope of this tangent line is δ, which is greater than the derivative of the power function, so that the inequality is valid $\forall|\sigma| > 1$.

Lemma 3 *Let $0 < \delta < 1$, define μ as:*

$$\mu = \max\left(\sqrt[1-\delta]{\frac{1}{\delta + \gamma(1-\delta)}}, \sqrt{\frac{5}{6}}\frac{1}{\gamma}\right) \tag{38}$$

Then $\forall|\sigma| > \mu$ the following conditions holds:

$$\delta|\sigma| + (1-\delta)|\tanh(\gamma\sigma)| \geq |\sigma|^\delta \tag{39}$$

Proof The bottom plot of Figure (2) displays the geometrical construction of the proposed inequality. In this case the new root can be bounded by means of the series expansion at $\sigma = 0$ of the hyperbolic tangent function:

$$\tanh(\gamma\sigma) = \gamma\sigma - \frac{\gamma^3\sigma^3}{3} + \frac{2\gamma^5\sigma^5}{15} + O(\sigma^6) \tag{40}$$

Therefore

$$|\tanh(\gamma\sigma)| > \gamma|\sigma| + \gamma^3|\sigma|^3\left(\frac{6\gamma^2|\sigma|^2 - 5}{15}\right) \tag{41}$$

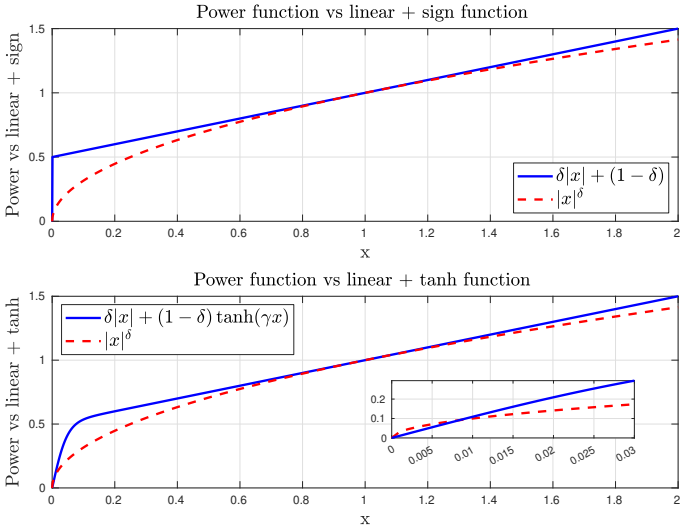

Fig. 2 Power function approximation.

Condition

$$|\sigma| \geq \sqrt{\frac{5}{6}}\frac{1}{\gamma} \tag{42}$$

implies that $6\gamma^2|\sigma|^2 - 5 \geq 0$ thus:

$$\delta|\sigma| + (1-\delta)|\tanh(\gamma\sigma)| > \delta|\sigma| + (1-\delta)\gamma|\sigma| \ \forall\sigma \geq \mu \tag{43}$$

Condition

$$|\sigma| \geq \sqrt[1-\delta]{\frac{1}{\gamma(1-\delta)}} \tag{44}$$

leads to:

$$\delta|\sigma| + (1-\delta)\gamma|\sigma| \geq |\sigma|^{\delta} \ \forall\sigma \geq \mu \tag{45}$$

which ends the proof.

Next, we introduce a theorem using the previous results to prove the convergence provided by *ASNSTA*.

Theorem 3 *Let c_1, c_2 and c_3 are positive parameters and assume that the following condition holds:*

$$p_2\alpha + 0.5 \geq \frac{(c_2(1-\delta) + 2^{\zeta}c_3)p_3\tanh(\gamma\mu)}{2^{\zeta}\Delta} \tag{46}$$

with μ given in (38), ζ given as:

$$\zeta = \frac{\delta + 1}{2} \tag{47}$$

In addition, let us define λ as:

$$\lambda = \frac{c_1}{2} + \frac{\delta c_2}{2^\zeta} \tag{48}$$

The compact set Ω_{η_3} defined as:

$$\Omega_{\eta_3} = \{\eta(t) \in \mathbb{R}^2 : |\sigma| < \mu \wedge |\omega| < c_3 |\tanh(\gamma\sigma)|\} \tag{49}$$

, which is a closed set including the origin of $\eta(t)$, is Finite Time Stable (FTS). The settling time can be estimated as:

$$T \leq \frac{2}{c_1(1-\delta)} \ln\left(\frac{c_1 V^{(\frac{1-\delta}{2})}(0) + c_2}{c_2}\right) \tag{50}$$

Proof Let's choose a Lyapunov candidate function:

$$V(\sigma) = \frac{1}{2}\sigma^2 \tag{51}$$

Condition (46) and equation (31) implies that:

$$\beta \geq \frac{c_2(1-\delta)}{2^\zeta} + c_3 \tag{52}$$

Application of (52) and (48) leads to:

$$\dot{V}(\sigma) \leq -\frac{c_1}{2}\sigma^2 - \frac{c_2}{2^\zeta}|\sigma|(\delta|\sigma| + (1-\delta)|\tanh(\gamma\sigma)|) - (c_3|\tanh(\gamma\sigma)| - |\omega|)|\sigma| \tag{53}$$

Condition $|\omega| < c_3|\tanh(\gamma\sigma)|$ implies that $(c_3|\tanh(\gamma\sigma)| - |\omega|)|\sigma| \geq 0$ which leads to:

$$\dot{V}(\sigma) \leq -\frac{c_1}{2}\sigma^2 - \frac{c_2}{2^\zeta}|\sigma|(\delta|\sigma| + (1-\delta)|\tanh(\gamma\sigma)|) \tag{54}$$

Lemma (3) implies that $\forall|\sigma(t)| > \mu$:

$$\dot{V}(\sigma) \leq -\frac{c_1}{2}\sigma^2 - \frac{c_2}{2^\zeta}|\sigma|^{\delta+1} \leq -c_1 V(\sigma) - c_2 V^\zeta(\sigma) \tag{55}$$

Because $0.5 < \zeta < 1$, application of Lemma (1) finalizes the proof.

3 Discretization and parameter settings.

It has been emphasized in publications such as [34, 48, 52, 53, 54, 55] that the discretization of continuous-time systems involving set values or fractional power functions should be carried out with care because:

- The chattering phenomenon is closely related to the discretization method.
- The properties related to set value and fractional power functions in the continuous analysis should be preserved in the discrete model.

In order to resolve these issues, it is common to replace the explicit discretization method with an implicit method, which provides higher stability to the integration process and eliminates chattering. In this research, since the functions being used are smooth, the approach is to use a simple semi-implicit discretization method to introduce parameter restrictions that will cancel the chattering.

3.1 Semi-implicit discretization.

The Backward Euler discretization method with fixed sampling time τ yields:

$$\sigma_{k+1} = \sigma_k - \tau(\lambda\sigma_k + \beta\tanh(\gamma\sigma_k) + \epsilon_k - d_k) \tag{56}$$

$$\epsilon_{k+1} = \epsilon_k + \tau(\frac{\lambda^2}{4}\sigma_k + \kappa\tanh(\gamma\sigma_k)) \tag{57}$$

A semi-implicit approximation can be obtained by replacing ϵ_k with ϵ_{k+1} in the expression of σ_{k+1}, which leads to:

$$\sigma_{k+1} = \sigma_k - \tau(\lambda\sigma_k + \beta\tanh(\gamma\sigma_k) + \epsilon_{k+1} - d_k) \tag{58}$$

so that:

$$\begin{aligned}\sigma_{k+1} &= \sigma_k(1-\tau\lambda) - \tau\beta\tanh(\gamma\sigma_k) - \tau^2(\frac{\lambda^2}{4}\sigma_k + \kappa\tanh(\gamma\sigma_k)) - \tau(\epsilon_k - d_k)\\ &= \sigma_k(1-\tau\lambda) - \tau\beta\tanh(\gamma\sigma_k) - \tau^2(\frac{\lambda^2}{4}\sigma_k + \kappa\tanh(\gamma\sigma_k)) - \tau\omega_k\end{aligned} \tag{59}$$

3.2 Parameter settings.

Taking into account the chattering resulting from the discretization process, as well as assuming a completely free noise system, we can create bounds for the parameters based on the discrete model. This choice involves a trade-off: on the one hand, it may be desirable to set these gains to high values in order to obtain a robust, fast response at steady state. Alternatively, they must not be too large, in order to prevent chattering at steady state. Hence, in this section we calculate the bounds for the gains λ, β, and γ that prevent chattering for a fixed sampling time τ.

Assumption 31 *Let's assume that the following holds:*

1. *Simulations are executed with fixed sampling time* τ.
2. $\tau\omega_k$ *is negligible in (59) when* $|\sigma_k| = \mu$.
3. $\tanh(\gamma\mu) \approx \gamma\mu$ *when* $|\sigma_k| = \mu$.

From Assumption 31 two restrictions are introduced in order to cancel the chattering caused by finite time discretization as follows:

$$(\lambda + \beta\gamma) < \frac{1}{2\tau} \tag{60}$$

$$(\frac{\lambda^2}{4} + \frac{\lambda}{2}\beta\gamma) < \frac{1}{2\tau^2} \tag{61}$$

These restrictions are defined so as not to result in a shift in the sign of σ_k at $|\sigma_k| = \mu$. Choosing

$$\beta\gamma = \lambda \tag{62}$$

the restriction

$$\lambda < \frac{1}{4\tau} \tag{63}$$

yields the desired condition. Depending on the application domain of the algorithm, the parameter γ can be selected in a variety of ways. In this study, we use the value that provides a good approximation of the set-value sign function by taking into account the fact that the application of an adaptive cut-off frequency means that λ, β and κ are adaptive gains. Let's choose γ as follows:

$$\gamma = \frac{1}{2\tau} \tag{64}$$

Therefore, from (62), β is given as:

$$\beta = 2\tau\lambda \tag{65}$$

3.3 Adaptive Cut-off frequency design.

Note that if the nonlinear terms in (7) are canceled, the transfer function from $d(t)$ to $\sigma(t)$ is given as:

$$G_{d\sigma}(s) = \frac{Z(s)}{D(s)} = \frac{s}{(s + \frac{\lambda}{2})^2} \tag{66}$$

which resembles the full-order transfer function obtained in [56] (*page 11*) for a second order system. Transfer function $G_{d\sigma}(s)$ implies that:

$$\lambda = 2\omega_c \tag{67}$$

where ω_c is chosen as the desired cut-off frequency. Applying (63), a bound for the application of the algorithm is:

$$\omega_{c_{max}} \leq \frac{1}{8\tau} \tag{68}$$

The frequency design approach allow us to introduce a modification that reduces the peaking phenomenon, which, as in the case of chattering, is related to variable module and frequency oscillations generated at the transient response of linear systems causing the well known overshooting problem. In order to obtain a soft adaptation of this parameter, several solutions can be provided. Between them, in this work we choose to adapt the value of the cut-off frequency as follows:

$$\omega_c(t) = \omega_{c_{min}} + (\omega_{c_{max}} - \omega_{c_{min}}) \frac{(1 + \tanh(t - 2.5t_s))}{2} \tag{69}$$

with t_s the desired settling time and $[\omega_{c_{min}}, \omega_{c_{max}}]$ are the chosen bounds of the adaptive cut-off frequency.

4 Smooth finite-time sliding mode control of second order systems.

Consider a second order system with dynamics given as:

$$\begin{aligned} \dot{x}_1(t) &= x_2(t) \\ \dot{x}_2(t) &= f(x) + bu(x) + d(t) \end{aligned} \tag{70}$$

such that the states must follow a reference trajectory given as $x_1^d(t)$, $x_2^d(t)$. Let:

$$\begin{aligned} e(t) &= x_1(t) - x_1^d(t) \\ \dot{e}(t) &= x_2(t) - x_2^d(t) \end{aligned} \tag{71}$$

An integral nonlinear sliding surface $\sigma(t)$ is defined as:

$$\sigma(t) = \dot{e}(t) + \lambda_e e(t) + \beta_e \tanh(\gamma_e e(t)) + \epsilon_e(t) \tag{72}$$

with

$$\dot{\epsilon}_e(t) = \frac{\lambda_e^2}{4} e(t) + \kappa_e \tanh(\gamma_e e) \tag{73}$$

and initial condition:

$$\epsilon_e(0) = -(\dot{e}(0) + \lambda_e e(0) + \beta_e \tanh(\gamma_e e(0))) \tag{74}$$

which implies that $\sigma(0) = 0$. The dynamics of $e(t)$ are given as:

$$\dot{e}(t) = -\lambda_e e(t) - \beta_e \tanh(\gamma_e e(t)) - \epsilon_e(t) - \sigma(t) \tag{75}$$

Let $d_e(t) = -\sigma(t)$. As a result, the dynamics of $e(t)$ and $\omega_e(t) = d_e(t) - \epsilon_e(t)$ are given as:

$$\begin{aligned} \dot{e}(t) &= -\lambda_e e(t) - \beta_e \tanh(\gamma_e e) + \omega_e(t) \\ \dot{\omega}_e(t) &= -\frac{\lambda_e^2}{4} e(t) - \kappa_e \tanh(\gamma_e e) + \dot{d}_e(t) \end{aligned} \tag{76}$$

which follows the *ASNSTA* approach. The derivative of $\sigma(t)$ is obtained as:

$$\dot{\sigma}_e(t) = f(x) + bu(x) + d(t) - \dot{x}_2^d(t) + \lambda_e \dot{e}(t) + \beta_e \gamma_e \operatorname{sech}^2(\gamma_e e)\dot{e}(t) - \dot{\epsilon}_e(t) \tag{77}$$

In order to achieve the sliding mode condition the control law is given as:

$$u(x) = -\frac{1}{b}\left[f(x) - \dot{x}_2^d(t) + u_\sigma(t) + u_e(t)\right] \tag{78}$$

with $u_e(t)$ and $u_\sigma(t)$ given as:

$$u_e(t) = \lambda_e \dot{e}(t) + \beta_e \gamma_e \operatorname{sech}^2(\gamma_e e)\dot{e}(t) + \dot{\epsilon}_e(t) \tag{79}$$

$$u_\sigma(t) = \lambda_\sigma s(t) + \beta_\sigma \tanh(\gamma_\sigma s) + \epsilon_\sigma(t) \tag{80}$$

where $\dot{\epsilon}_\sigma(t)$ is:

$$\dot{\epsilon}_\sigma(t) = \frac{\lambda_\sigma^2}{4}\sigma(t) + \kappa_\sigma \tanh(\gamma_\sigma \sigma) \tag{81}$$

with initial condition:

$$\epsilon_\sigma(0) = 0 \tag{82}$$

As a result, the dynamics of $\sigma(t)$ and $\omega_\sigma(t) = d(t) - \epsilon_\sigma(t)$ are given as:

$$\begin{aligned} \dot{\sigma}(t) &= -\lambda_\sigma \sigma(t) - \beta_\sigma \tanh(\gamma_\sigma \sigma) + \omega_\sigma(t) \\ \dot{\omega}_\sigma(t) &= -\frac{\lambda_\sigma^2}{4}\sigma(t) - \kappa_\sigma \tanh(\gamma_\sigma \sigma) + \dot{d}(t) \end{aligned} \tag{83}$$

which follows the *ASNSTA* approach.

5 Case studies: numerical simulations

In the simulation section, *ASNSTA* is compared to the smooth second-order sliding mode control (*SOSMC*) presented in [57] in the case of a variable-length pendulum whose dynamics are given by:

$$\ddot{\theta}(t) = -2\frac{\dot{R}}{R}\dot{\theta}(t) - g\frac{1}{R}\sin(\theta) + \frac{1}{mR^2}u \tag{84}$$

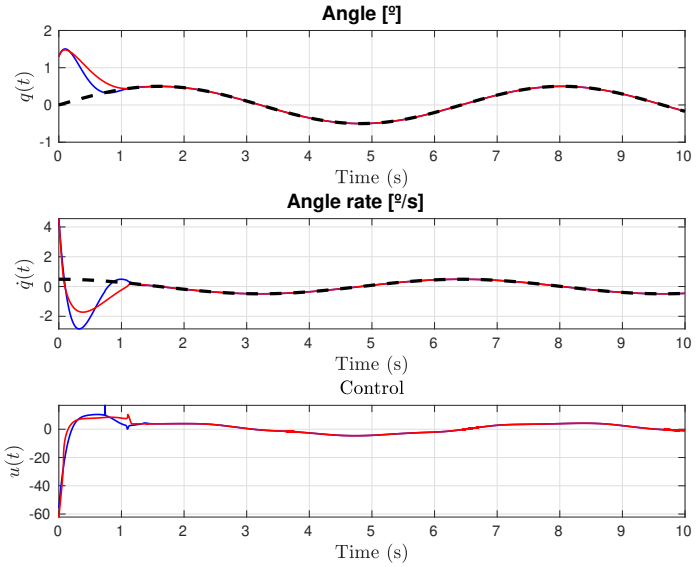

Fig. 3 Case 1: unperturbed system ($d(t) = 0$). States and control: time courses for $t \in [0, 10]$. Dashed black lines: Reference; Red lines: Results obtained with *SOSMC*; Blue lines: Results obtained with *ASNSTA*.

where θ is the oscillation angle (rad), $m = 1kg$ is the mass of the pendulum, $g = 9.81m/s^2$ is the gravitational constant, R is the distance (m) from the axis of rotation of the pendulum to the mass given as:

$$R(t) = 1 - 0.1\sin(5t) \tag{85}$$

and u is the control input (N m). The desired reference to follow is given as:

$$\theta_d = 0.5sin(0.5t) \text{ rad} \tag{86}$$

In order to apply *ASNSTA* the following steps must be followed:

1. Choose the adaptive cut-off frequency as follows:

$$\begin{aligned}
\omega_{c_{min}} &= 1 \\
\omega_{c_{max}} &= \frac{1}{10\tau} \\
\omega_c(t) &= \omega_{c_{min}} + (\omega_{c_{max}} - \omega_{c_{min}})\frac{(1 + \tanh(t - 2.5t_s))}{2}
\end{aligned}$$

with $t_s = 1s$ in order to be the same as the settling time obtained with *SOSMC* in the unperturbed case scenario.

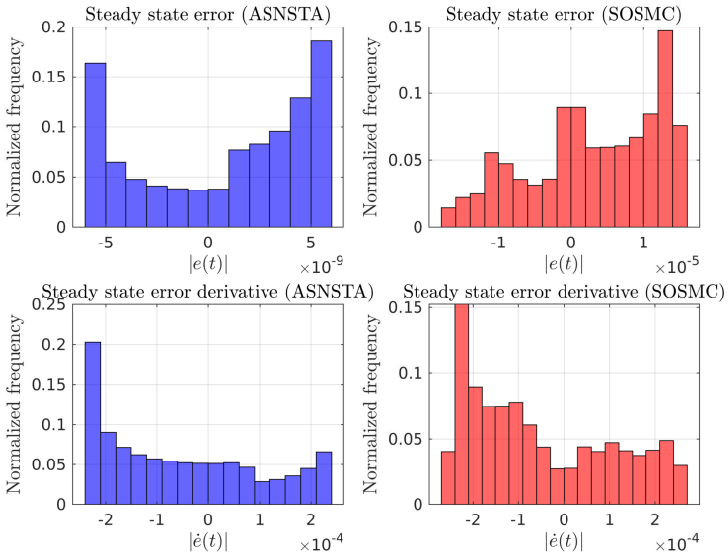

Fig. 4 Case 1: unperturbed system ($d(t) = 0$). Histogram of steady state error for $t \in [5, 10]$.Red: Results obtained with *SOSMC*; Blue: Results obtained with *ASNSTA*.

2. Choose the parameters to generate $u_e(t)$ and $u_\sigma(t)$ in (78) as follows:

$$\gamma_e = \gamma_\sigma = \frac{1}{2\tau}$$
$$\lambda_e = \lambda_\sigma = 2\omega_c$$
$$\beta_e = \beta_\sigma = \frac{\lambda_e}{\gamma_e}$$
$$p_2 = \frac{5\lambda_e^2 + 4}{2\lambda_e^3}$$
$$\kappa_e = \kappa_\sigma = \frac{\beta_e}{2p_2}$$

Therefore, the algorithm parameters and its adaptation can be easily obtained directly from a frequency domain approach taken account of the sampling time used to simulate the model.

5.1 Case 1: unperturbed system

In this case both controllers are simulated with $d(t) = 0$ and sampling $\tau = 0.001$ s. Figure 3 shows the evolution of states and control signals, where the settling time and the trajectory is quite similar in both solutions. In contrast, ASNSTA provides improved accuracy at steady state, as illustrated in Figure 4, which presents the normalized distribution of the error and its derivative for $t \in [5, 10]$.

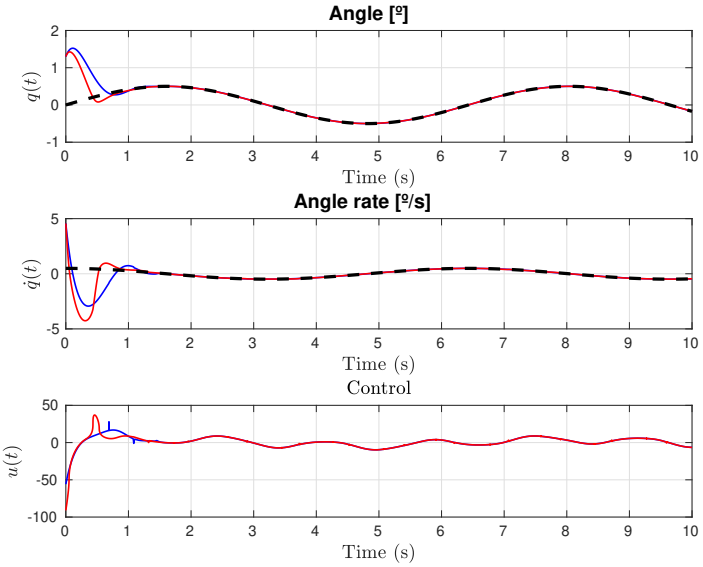

Fig. 5 Case 2: cosine perturbation ($d(t) = 5.15\cos(3.75t)$). States and control: time courses for $t \in [0, 10]$. Dashed black lines: Reference; Red lines: Results obtained with $SOSMC$; Blue lines: Results obtained with $ASNSTA$.

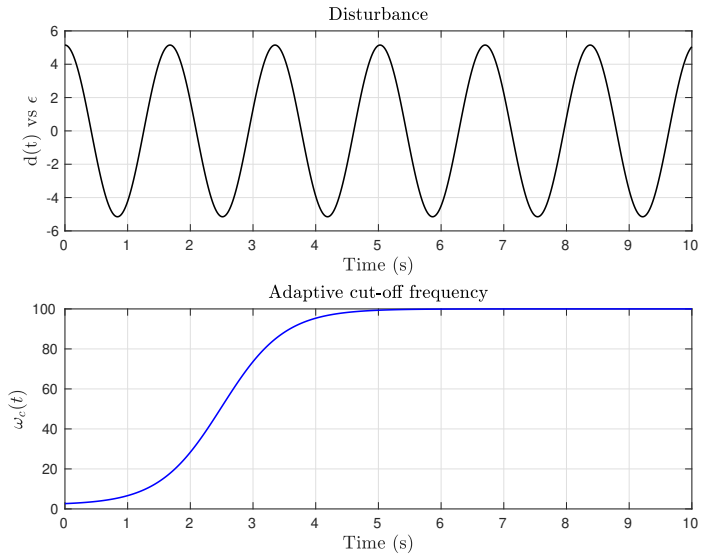

Fig. 6 Case 2: cosine perturbation perturbation ($d(t) = 5.15\cos(3.75t)$). Disturbance and adaptive cut-off frequency.

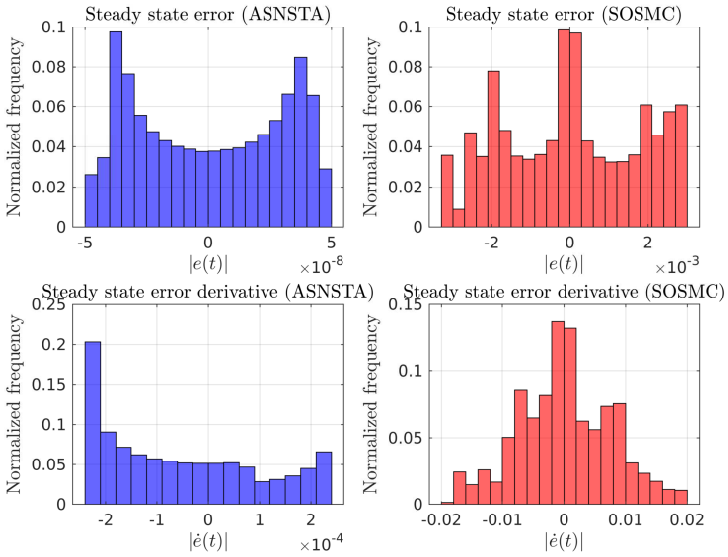

Fig. 7 Case 2: cosine perturbation perturbation ($d(t) = 5.15\cos(3.75t)$). Histogram of steady state error.Red: Results obtained with *SOSMC*; Blue: Results obtained with *ASNSTA*.

5.2 Case 2: cosine disturbance

In this case te disturbance is given as $d(t) = 5.15\cos(3.75t)$ and the sampling used is $\tau = 0.001$ s.

Figure 5 shows the evolution of states and control signals, demonstrating that the results are comparable to those obtained in the unperturbed case, but only *ASNSTA* is able to maintain the unperturbed trajectory as well as a high steady state accuracy.

Illustration of the disturbance and the adjustment of the cut-off frequency design parameter is presented in Figure 5. The soft adaptation used for the cut-off frequency allows the rejection of large control values at the initial instant when the error is large, while generating large gains at steady state, contributing to the improvement of the accuracy obtained and the cancellation of the overshooting. The normalized distribution of the error and its derivative for $t \in [5, 10]$ can be consulted in Figure 7.

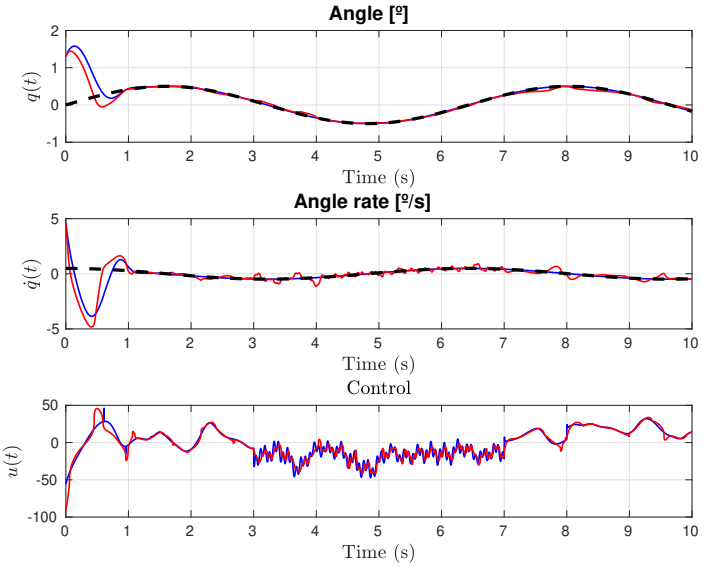

Fig. 8 Case 3: variable module and frequency perturbation. States and control: time courses for $t \in [0, 10]$. Dashed black lines: Reference; Red lines: Results obtained with $SOSMC$; Blue lines: Results obtained with $ASNSTA$.

5.3 Case 3: variable module and frequency disturbance

In this case the control algorithms are tested using a variable module disturbance that includes impulsive and high frequency channels given as:

$$d(t) = D[\cos(\omega_d t) + 0.83\sin(2.85\omega_d t - 0.14) + 1.23\cos(1.72\omega_d t + 0.26) + 0.65\sin(1.91\omega_d t + 0.36)e^{\cos(2.21\omega_d t + 0.13)}] + d_1(t) + d_2(t) \quad (87)$$

where:

$$d_1(t) = \begin{cases} 2.75D + 1.34D\cos(23.4\omega_d t + 0.46) & \text{if } 3 < t < 7 \\ 0 & \text{otherwise} \end{cases} \quad (88)$$

and

$$d_2(t) = \begin{cases} -3.5D & \text{if } 7 < t < 10 \\ 0 & \text{otherwise} \end{cases} \quad (89)$$

with

$$D = 5.15 \quad (90)$$

$$\omega_d = 3.75\frac{rad}{s} \quad (91)$$

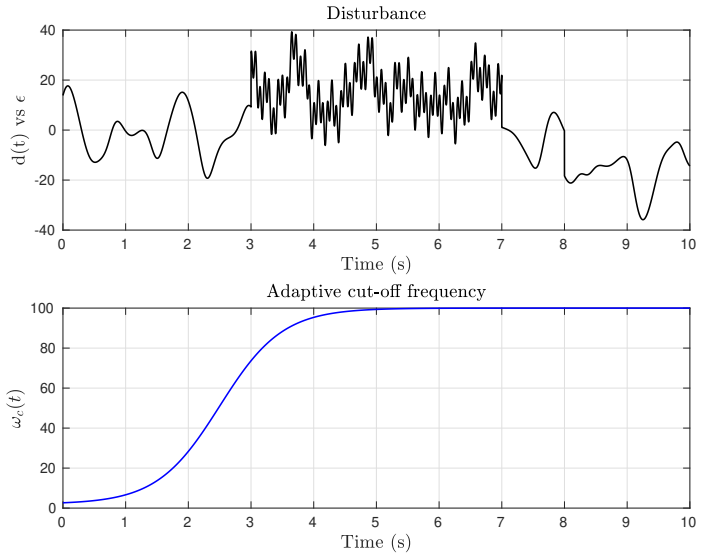

Fig. 9 Case 3: variable module and frequency perturbation. Disturbance and adaptive cut-off frequency.

Figures 5, 9 and 10 shows the evolution of states and control signals, the disturbance, the adaption value of the cut-off frequency and the normalized distribution of the steady state error. The performance obtained with *ASNSTA* is similar to the previous cases with an invariant state trajectory and with an small reduction in the steady state accuracy.

5.4 Case 4: unperturbed system with $\tau = [0.1, 0.01]$

In this case the unperturbed scenario is considered but using larger values of the sampling time: $\tau = 0.01$ and $\tau = 0.1$.

Figures 11 and 12 illustrate the results obtained with larger sampling time periods. As it can be seen, *ASNSTA* cancels the chattering that appears in *SOSMC*, while increasing τ value. In order to achieve this behaviour, the adaptive algorithm decreases the top cut-off frequency, causing the response to become slower, as it can be appreciated in the figures.

6 Discussion and conclusions

In this study, an approach for developing an adaptive integral sliding mode procedure to design controllers for nonlinear second order systems is proposed, such that the solution employs adaptive gains that alter the sliding surface's

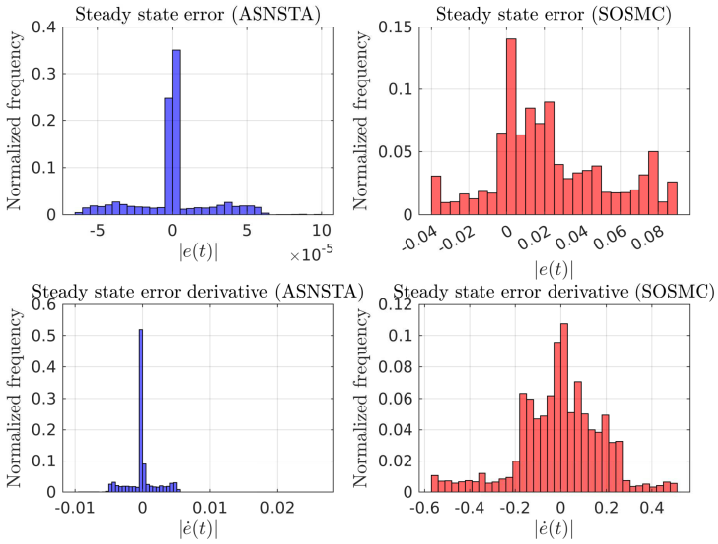

Fig. 10 Case 3: variable module and frequency perturbation. Histogram of steady state error.Red: Results obtained with *SOSMC*; Blue: Results obtained with *ASNSTA*.

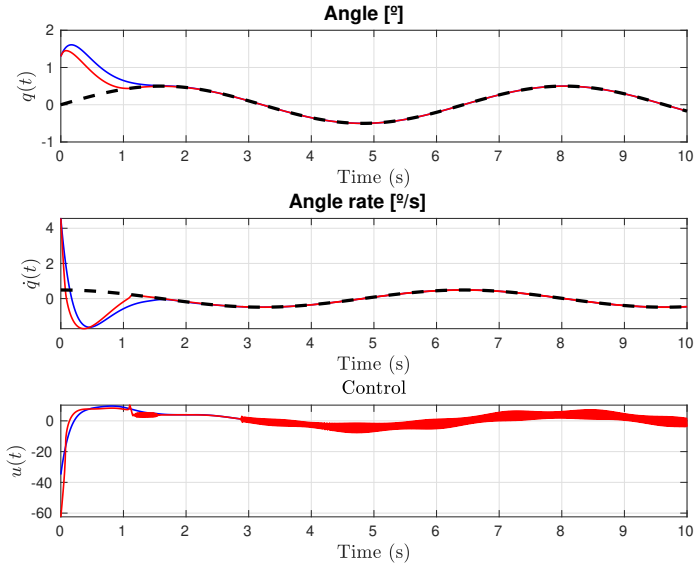

Fig. 11 Case 1: unperturbed system ($d(t) = 0$) and $\tau = 0.01$ s. States and control: time courses for $t \in [0, 10]$. Dashed black lines: Reference; Red lines: Results obtained with *SOSMC*; Blue lines: Results obtained with *ASNSTA*.

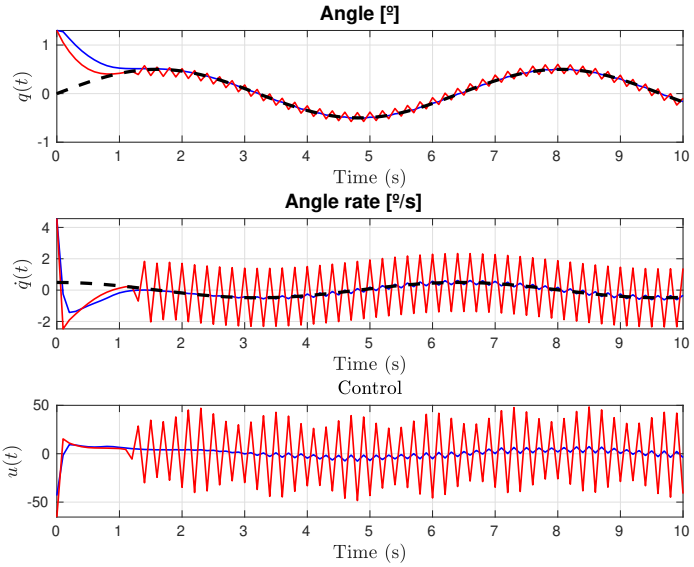

Fig. 12 Case 1: unperturbed system ($d(t) = 0$) and $\tau = 0.1$ s. States and control: time courses for $t \in [0, 10]$. Dashed black lines: Reference; Red lines: Results obtained with *SOSMC*; Blue lines: Results obtained with *ASNSTA*.

dumping properties based on a cut-off frequency domain technique. This adaptation generates a low/high gain profile that allows to overcome the requirement for large control inputs at initial conditions, while enabling a higher gain at steady state to avoid two undesirable phenomena: peaking and chattering.

As a restriction, we introduce an upper bound on the derivative of the unknown term in the dynamic equation (Δ). This method has the advantage of being robust to overestimations of Δ, so performance is not severely affected if this bound is not accurately known. However, choosing an overly large value might result in oscillations in the response of the estimation error.

Analyses of numerical simulations indicate that the proposed algorithm is capable of achieving the desired performance with time-varying references and external disturbances.

Especially when the model is noisy, the cut-off frequency should be lowered in order to reduce the impact of high frequency components on the generation of the control law, unless some prior filtering of the observer signals has been performed. In future work, the use of nonlinear high-frequency filtering techniques for attenuating the time delay caused by noisy signals, as well as the scaling of the technique to deal with more complex dynamic systems, will be areas of interest.

Competing Interests

The authors declare that they have no known competing financial interests or personal relationships that could have appeared to influence the work reported in this paper.

Author Contributions

José Antonio González-Prieto: Conceptualization, Investigation, Methodology (observer design), Software (numerical simulations), Formal analysis, Writing – original draft, Writing – Review & Editing.

Funding

J. A. González-Prieto acknowledges funding from the Defense University Center at the Spanish Naval Academy, Spanish Ministry of Defense, TRABODIT project (PICUD-2021-01).

Code availability

The MATLAB code of the numerical simulations presented in this paper is available at:
`https://github.com/jagprieto/asnsta_second_order_systems/`.

References

1. J-JE Slotine, J Kand Hedrick, and Eduardo A Misawa. On sliding observers for nonlinear systems. *Journal of Dynamic Systems, Measurement, and Control*, 109, 1987.
2. C. Edwards and S. Spurgeon. Sliding mode control: Theory and applications. *CRC press*, 1998.
3. Arie Levant. Robust exact differentiation via sliding mode technique. *Automatica*, 34(3):379–384, 1998.
4. S. K. Spurgeon C. Edwards and R. J. Patton. Sliding mode observers for fault detection and isolation. *Automatica*, 36(4):541–55, 2000.
5. J. Guldner V. Utkin and J. Shi. Sliding mode control in electro-mechanical systems. *CRC press*, 2009.
6. Y. Xinghuo Y. Feng and M. Zhihong. Non-singular terminal sliding mode control of rigid manipulators. *Automatica*, 38(12):2159–2167, 2002.
7. D. Zhao Y. Hao, J. Yi and D. Qian. Robust control using incremental sliding mode for underactuated systems with mismatched uncertainties. *American Control Conference, IEEE 2008*, pages 532–537, 2008.

8. Jianxing Liu, Salah Laghrouche, Mohamed Harmouche, and Maxime Wack. Adaptive-gain second-order sliding mode observer design for switching power converters. *Control Engineering Practice*, 30:124–131, 2014.
9. Jun Yang, Shihua Li, and Xinghuo Yu. Sliding-mode control for systems with mismatched uncertainties via a disturbance observer. *IEEE Transactions on industrial electronics*, 60(1):160–169, 2012.
10. J. P. VS Cunha L. Hsu, T. R. Oliveira and L. Yan. Adaptive unit vector control of multivariable systems using monitoring functions. *International Journal of Robust and Nonlinear Control*, 29(3):583–600, 2019.
11. Yi Xiong and Mehrdad Saif. Sliding mode observer for nonlinear uncertain systems. *IEEE transactions on automatic control*, 46(12):2012–2017, 2001.
12. J Barbot, M Djemai, and T Boukhobza. Sliding mode observers. *Sliding mode control in engineering*, 11:33, 2002.
13. Hassan Hammouri and M Farza. Nonlinear observers for locally uniformly observable systems. *ESAIM: Control, optimisation and calculus of Variations*, 9:353–370, 2003.
14. Thierry Floquet, Chris Edwards, and Sarah K Spurgeon. On sliding mode observers for systems with unknown inputs. *International Journal of Adaptive Control and Signal Processing*, 21(8-9):638–656, 2007.
15. Chee Pin Tan, Xinghuo Yu, and Zhihong Man. Terminal sliding mode observers for a class of nonlinear systems. *Automatica*, 46(8):1401–1404, 2010.
16. Saleh Mobayen. An adaptive fast terminal sliding mode control combined with global sliding mode scheme for tracking control of uncertain nonlinear third-order systems. *Nonlinear Dynamics*, 82(1):599–610, 2015.
17. Shihong Ding, Ju H Park, and Chih-Chiang Chen. Second-order sliding mode controller design with output constraint. *Automatica*, 112:108704, 2020.
18. Ankush Chakrabarty, Ann E Rundell, Stanislaw H Zak, Fanglai Zhu, and Gregery T Buzzard. Unknown input estimation for nonlinear systems using sliding mode observers and smooth window functions. *SIAM Journal on Control and Optimization*, 56(5):3619–3641, 2018.
19. Q. Wu M. Chen and R. Cui. Terminal sliding mode tracking control for a class of siso uncertain nonlinear systems. *ISA transactions*, 52(2):198–206, 2013.
20. X. D. Liu W. Wang and J. Q. Yi. Structure design of two types of sliding-mode controllers for a class of under-actuated mechanical systems. *IET Control Theory & Applications*, 1(1):16388–172, 2007.
21. Jianmin Wang, Yunjie Wu, and Xiaomeng Dong. Recursive terminal sliding mode control for hypersonic flight vehicle with sliding mode disturbance observer. *Nonlinear Dynamics*, 81(3):1489–1510, 2015.
22. Ha Le Nhu Ngoc Thanh, Nguyen Xuan Mung, Ngoc Phi Nguyen, Nguyen Thanh Phuong, and other. Perturbation observer-based robust control using a multiple sliding surfaces for nonlinear systems with influences of matched and unmatched uncertainties. *Mathematics*, 8(8):1371, 2020.

23. Yuan-Xin Li and Guang-Hong Yang. Adaptive integral sliding mode control fault tolerant control for a class of uncertain nonlinear systems. *IET Control Theory & Applications*, 12(13):1864–187, 2018.
24. Dong Liu and Guang-Hong Yang. Prescribed performance model-free adaptive integral sliding mode control for discrete-time nonlinear systems. *IEEE transactions on neural networks and learning systemss*, 30(7):2222–2230, 2018.
25. Khalid A Alattas, Saleh Mobayen, Sami Ud Din, Jihad H Asad, Afef Fekih, Wudhichai Assawinchaichote, and Mai The Vu. Design of a non-singular adaptive integral-type finite time tracking control for nonlinear systems with external disturbances. *IEEE Access*, 9:102091–102103, 2021.
26. Christopher Edwards and Yuri B Shtessel. Adaptive continuous higher order sliding mode control. *Automatica*, 65:183–190, 2016.
27. Yong Feng, Fengling Han, and Xinghuo Yu. Chattering free full-order sliding-mode control. *Automatica*, 50(4):1310–1314, 2014.
28. Bijnan Bandyopadhyay, Fulwani Deepak, and Kyung-Soo Kim. *Sliding mode control using novel sliding surfaces*, volume 392. Springer, 2009.
29. José Antonio González, Antonio Barreiro, Sebastián Dormido, and Alfonso Banos. Nonlinear adaptive sliding mode control with fast non-overshooting responses and chattering avoidance. *Journal of the Franklin Institute*, 354 (7):2788–2815, 2017.
30. José Antonio González, Antonio Barreiro, and Sebastián Dormido. A practical approach to adaptive sliding mode control. *International Journal of Control, Automation and Systems*, 17(10):2452–2461, 2019.
31. Juntao Fei and Hongfei Ding. Adaptive sliding mode control of dynamic system using rbf neural network. *Nonlinear Dynamics*, 70(2):1563–1573, 2012.
32. Muhammad Umair Khan and Tolgay Kara. Adaptive type-2 neural fuzzy sliding mode control of a class of nonlinear systems. *Nonlinear Dynamics*, 101(4):2283–2297, 2020.
33. Andrey Polyakov. *Generalized homogeneity in systems and control*. Springer, 2020.
34. Mohammad Rasool Mojallizadeh, Bernard Brogliato, and Vincent Acary. Time-discretizations of differentiators: Design of implicit algorithms and comparative analysis. *International Journal of Robust and Nonlinear Control*, 2021.
35. Thierry Floquet and Jean-Pierre Barbot. Super twisting algorithm-based step-by-step sliding mode observers for nonlinear systems with unknown inputs. *International journal of systems science*, 38(10):803–815, 2007.
36. Alejandro Dávila, Jaime A Moreno, and Leonid Fridman. Variable gains super-twisting algorithm: A lyapunov based design. In *Proceedings of the 2010 American Control Conference*, pages 968–973. IEEE, 2010.
37. Jaime A Moreno and Marisol Osorio. Strict lyapunov functions for the super-twisting algorithm. *IEEE transactions on automatic control*, 57(4): 1035–1040, 2012.

38. Shyam Kamal, Asif Chalanga, Jaime A Moreno, L Fridman, and Bijnan Bandyopadhyay. Higher order super-twisting algorithm. In *2014 13th International Workshop on Variable Structure Systems (VSS)*, pages 1–5. IEEE, 2014.
39. Richard Seeber, Martin Horn, and Leonid Fridman. A novel method to estimate the reaching time of the super-twisting algorithm. *IEEE Transactions on Automatic Control*, 63(12):4301–4308, 2018.
40. Jianping Guo, Renquan Lu, Deyin Yao, and Qi Zhou. Implementation of the load frequency control by two approaches: variable gain super-twisting algorithm and super-twisting-like algorithm. *Nonlinear Dynamics*, 93(3): 1073–1086, 2018.
41. Jiahao Yuan, Shihong Ding, and Keqi Mei. Fixed-time sosm controller design with output constraint. *Nonlinear Dynamics*, 102(3):1567–1583, 2020.
42. Juntao Fei and Zhilin Feng. Adaptive fuzzy super-twisting sliding mode control for microgyroscope. *Complexity*, 2019, 2019.
43. Stefan Koch and Markus Reichhartinger. Discrete-time equivalents of the super-twisting algorithm. *Automatica*, 107:190–199, 2019.
44. HJ Sussmann and PV Kokotovic. The peaking phenomenon and the global stabilization of nonlinear systems. *IEEE Transactions on automatic control*, 36(4):424–440, 1991.
45. Arie Levant. Chattering analysis. *IEEE transactions on automatic control*, 55(6):1380–1389, 2010.
46. Wameedh Riyadh Abdul-Adheem, Ibraheem Kasim Ibraheem, Amjad J Humaidi, Ahmed Alkhayyat, Rami A Maher, Ahmed Ibraheem Abdulkareem, and Ahmad Taher Azar. Design and analysis of a novel generalized continuous tracking differentiator. *Ain Shams Engineering Journal*, page 101656, 2021.
47. José Antonio González-Prieto and Alejandro F Villaverde. Smooth non linear high gain observers for a class of dynamical systems. *IEEE Access*, pages 1–1, 2021.
48. Bernard Brogliato, Andrey Polyakov, and Denis Efimov. The implicit discretization of the supertwisting sliding-mode control algorithm. *IEEE Transactions on Automatic Control*, 65(8):3707–3713, 2019.
49. Xiaogang Xiong, Zhichao Liu, Shyam Kamal, and Shanhai Jin. Discrete-time super-twisting observer with implicit euler method. *IEEE Transactions on Circuits and Systems II: Express Briefs*, 68(4):1288–1292, 2020.
50. D Coutinho, Alejandro Vargas, C Feudjio, Micaela Benavides, and A Vande Wouwer. A robust approach to the design of super-twisting observers–application to monitoring microalgae cultures in photobioreactors. *Computers & Chemical Engineering*, 121:46–56, 2019.
51. Shuanghe Yu, Xinghuo Yu, Bijan Shirinzadeh, and Zhihong Man. Continuous finite-time control for robotic manipulators with terminal sliding mode. *Automatica*, 41(11):1957–1964, 2005.
52. Mohammad Rasool Mojallizadeh, Bernard Brogliato, and Vincent Acary. *Discrete-time differentiators: design and comparative analysis*. INRIA,

2020.
53. Bernard Brogliato and Andrey Polyakov. Digital implementation of sliding-mode control via the implicit method: A tutorial. *International Journal of Robust and Nonlinear Control*, 31(9):3528–3586, 2021.
54. Ryo Kikuuwe, Rainhart Pasaribu, and Gyuho Byun. A first-order differentiator with first-order sliding mode filtering. *IFAC-PapersOnLine*, 52 (16):771–776, 2019.
55. Gyuho Byun and Ryo Kikuuwe. An improved sliding mode differentiator combined with sliding mode filter for estimating first and second-order derivatives of noisy signals. *International Journal of Control, Automation and Systems*, 18(12):3001–3014, 2020.
56. Hassan K Khalil and Laurent Praly. High-gain observers in nonlinear feedback control. *International Journal of Robust and Nonlinear Control*, 24(6):993–1015, 2014.
57. Panitnart Chawengkrittayanont, Chutiphon Pukdeboon, Suwat Kuntanapreeda, and Elvin J Moore. Smooth second-order sliding mode controller for multivariable mechanical systems. *SN Applied Sciences*, 3(10): 1–18, 2021.